

compared to unity. While E_{12} does enter x quadratically, the exact value used is not very important unless it is small enough to give x less than, say, unity. The insensitivity of $1 - \phi_0(x)$ to variation in x when $x \gg 1$ is simply the result of the rapid fall-off of the Boltzmann factor $\exp(-y)$ as compared to $P_R(y)$. This behavior was shown in Figure 2 and discussed in section III.

References and Notes

- (1) L. L. Lohr, Jr., *J. Am. Chem. Soc.*, preceding paper in this issue.
- (2) J. J. McGarvey and J. Wilson, *J. Am. Chem. Soc.*, **97**, 2531 (1975). The ligand abbreviated "dpp" is 1,3-bis(diphenylphosphino)propane.
- (3) L. Landau, *Phys. Z. Sowjetunion*, **2**, 46 (1932).
- (4) C. Zener, *Proc. R. Soc. London, Ser. A*, **137**, 696 (1932); **140**, 660 (1933).
- (5) H. Eyring, J. Walter, and G. E. Kimball, "Quantum Chemistry", Wiley, New York, N.Y., 1944, pp 326-330.
- (6) C. A. Coulson and K. Zalewski, *Proc. R. Soc. London, Ser. A*, **268**, 437 (1962).
- (7) (a) E. E. Nikitin, "Theory of Thermally Induced Gas Phase Reactions", Indiana University Press, Bloomington, Ind., 1966, pp 65-74; (b) "Theory of Elementary Atomic and Molecular Processes in Gases", Clarendon

- Press, Oxford, 1974, pp 99-178; (c) *Adv. Chem. Phys.*, **28**, 317 (1975).
- (8) M. S. Child, *Mol. Phys.*, **20**, 171 (1971).
- (9) (a) W. R. Thorson, J. B. Delos, and S. A. Boorstein, *Phys. Rev. Sect. A*, **4**, 1052 (1971); (b) J. B. Delos and W. R. Thorson, *ibid.*, **6**, 728 (1972).
- (10) (a) J. C. Tully and R. K. Preston, *J. Chem. Phys.*, **55**, 562 (1971); (b) J. C. Tully, *ibid.*, **61**, 61 (1974).
- (11) R. Rosen, "Dynamical Systems Theory in Biology", Vol. I, "Stability Theory and Its Applications", Wiley-Interscience, New York, N.Y., 1970.
- (12) E. K. Grimmelmann and L. L. Lohr, Jr., *Chem. Phys. Lett.*, in press.
- (13) B. J. Zwolinski and H. Eyring, *J. Am. Chem. Soc.*, **69**, 2702 (1947).
- (14) J. Z. Hearon, *Bull. Math. Biophys.*, **15**, 121 (1953).
- (15) J. Wei and C. Prater, *Adv. Catal.*, **13**, 203 (1962).
- (16) C. D. Thorn, *Bull. Math. Biophys.*, **34**, 277 (1972).
- (17) J. Z. Hearon, *Ann. N.Y. Acad. Sci.*, **108**, 36 (1963).
- (18) J. Wei and J. C. W. Kuo, *Ind. Eng. Chem., Fundam.*, **8**, 114 (1969).
- (19) E. Teller, *J. Phys. Chem.*, **41**, 109 (1937).
- (20) N. Rosen and C. Zener, *Phys. Rev.*, **40**, 502 (1932).
- (21) T. R. Dinterman and J. B. Delos, *Phys. Rev. Sect. A*, **15**, 463, 475 (1977), and references cited therein.
- (22) Thermally averaged Landau-Zener rate constants are presented in systematic graphical and tabular form in terms of reduced variables by M. B. Faist and R. B. Bernstein, *J. Chem. Phys.*, **64**, 3924 (1976); **66**, 5831 (1977).
- (23) C. T. Zahn, *Phys. Rev.*, **52**, 67 (1937).
- (24) O. Laporte, *Phys. Rev.*, **52**, 72 (1937).
- (25) H. C. Torrey, *Phys. Rev.*, **59**, 293 (1941).
- (26) M. Abramowitz, *J. Math. Phys.*, **32**, 188 (1953).

Resonance Raman Spectra of Cobalt(II)-Imidazole Complexes: Analogues of the Binding Site of Cobalt-Substituted Zinc Proteins

Simon Salama and Thomas G. Spiro*

Contribution from the Department of Chemistry, Princeton University, Princeton, New Jersey 08540. Received June 16, 1977

Abstract: Raman spectra, excited in the visible and near-ultraviolet (363.8 nm) regions, are reported for imidazole (ImH) and its N_1 and C_2 deuterated derivatives, and for several cobalt(II) complexes, chosen as analogues for the coordination group of zinc (cobalt) proteins $\text{Co}(\text{ImH})_4^{2+}$, $\text{Co}(\text{ImH})_2\text{Cl}_2$, $\text{Co}(\text{Im})_4^{2-}$, $\text{Co}(\text{his})_2$, and $\text{Co}(\text{his})_2^{2-}$ (his = histidinate), as well as N_1 -methyl, C_2 -methyl, and N_1 and C_2 deuterated analogues. Excitation in the visible absorption band enhances cobalt-ligand modes of the tetrahedral complexes. The intensity patterns suggest a vibronic mixing mechanism with charge-transfer upper states. The cobalt-imidazole frequencies suggest unusual strength for the Co-ImH bond in $\text{Co}(\text{ImH})_4^{2+}$, perhaps reflecting hydrogen bonding to the solvent. Imidazole ring modes are reassigned on the basis of corrected deuteration data. Frequency shifts on binding to Co^{2+} are unremarkable. However, the most intense band, at 1255 cm^{-1} , shifts significantly upon N_1 deuteration when complexed but not when free, and may therefore serve as a marker for cobalt-bound imidazole in proteins. The complexed ring modes are not enhanced in the visible but show significant enhancement in the near UV.

Zinc is a relatively abundant element in biological organisms, and plays an essential role in a large number of enzymatic reactions.¹ The structure of the zinc binding site has been elucidated for a growing list of proteins by x-ray crystallography. The structural aspects of catalysis are of great current interest for these enzymes. Zinc(II) being a d^{10} ion provides few spectroscopic signatures for the monitoring of structure. It can be substituted with cobalt(II) (d^7), however, with retention of at least partial enzymatic activity.² The resulting cobalt enzymes give characteristic visible (ligand-field) absorption spectra.

Resonance Raman spectroscopy affords a selective probe of chromophore structure. Vibrations which are coupled to the resonant electronic transition are subject to enhancement of their Raman intensity. The frequencies and intensities of the Raman bands are sensitive to structural changes occurring at the chromophore. In principle, resonance Raman spectra of cobalt-substituted enzymes could provide a vibrational sig-

nature of the active site. The experiment was tried by Loehr and co-workers,³ without positive results, but their available laser wavelengths were far from resonance. In view of recent reports of substantial Raman enhancement of cobalt-ligand stretching modes in resonance with the visible absorption bands of tetrahedral cobalt(II) complexes,⁴ the cobalt enzymes bear reexamination.

The most common zinc active-site ligand is imidazole. Three imidazoles are bound to zinc in carbonic anhydrase,⁵ two in carboxypeptidase⁶ and thermolysin,⁷ and one in liver alcohol dehydrogenase.⁸ It is therefore of importance to define the Raman characteristics of cobalt(II) imidazole complexes. Yoshida et al. have published a Raman study of such complexes,³ which was, however, limited to the high-frequency ligand modes, and to excitation with blue and green laser lines. In the present work we have focused on resonance effects observable in the red and the near-ultraviolet regions of the spectrum. The former provides selective enhancement of co-

Table I. Cobalt-Ligand Frequencies (cm⁻¹)

	$\nu_{\text{Co-Im(s)}}$	$\nu_{\text{Co-Im(as)}}$	$\nu_{\text{Co-Cl(s)}}$	$\nu_{\text{Co-Cl(as)}}$	$\nu_{\text{Co-NH}_2}$
Co(ImH) ₂ Cl ₂	232	274	305	339	
Co(2MeImH) ₂ Cl ₂	220	267	302		
Co(py) ₂ Cl ₂ ^a		252	304	344	
Co(2MeImH) ₄ ²⁺		270			
Co(1MeIm) ₄ ²⁺		280			
Co(ImH) ₄ ²⁺		301			
Co(Im-D) ₄ ²⁺		296			
Co(Im ⁻) ₄ ²⁻		306			
Co(his) ₂ ²⁻		305			366 (356 ND ₂)

^a From ref 14.

balt-ligand modes, while the latter provides high sensitivity for the monitoring of imidazole ring modes. We have also used deuterium exchange to confirm assignments of the latter.

Experimental Section

Imidazole and L-histidine free base were purchased from Sigma, CoCl₂ anhydrous was purchased from Matheson Coleman and Bell, and 2-methylimidazole and acetone-*d*₆ from Aldrich, and all were used without further purification.

Co(ImH)₄(ClO₄)₂ and the 2-Me-ImH analogue were prepared as reported by Davis and Smith.⁹ Co(ImH)₂Cl₂ was prepared according to Eilbeck and co-workers.^{10a} Co(histidinate)₂²⁻ and Co(Im)₄²⁻ were prepared according to Morris and Martin.¹¹ For these complexes the ratios Co:histidine and Co:Im were 1:4 and 1:1000, respectively. Care was taken to exclude oxygen from these two complexes.

All the spectra were taken in a spinning cell, using a Spectra Physics 170 Ar⁺ laser, with UV optics, and a Coherent Radiation Model 490 dye laser with Rhodamine 6-G and Na-Fluorescein dyes. The spectra were recorded with a Spex 1401 spectrometer with photon counting electronics. Absorption spectra were obtained with a Cary 118 spectrometer.

Results and Discussion

Cobalt(II) imidazole complexes were chosen with a view toward evaluating the possibilities for monitoring the coordination group of cobalt-substituted zinc proteins using visible or near-UV RR spectroscopy. Unfortunately no exact analogues have yet been synthesized for the known protein binding sites. These contain a bound water molecule plus three imidazole ligands (carbonic anhydrase⁵), or two imidazole and one carboxylate ligands (carboxypeptidase⁶ and thermolysin⁷) or one imidazole and two cysteine ligands (liver alcohol dehydrogenase⁸). The geometry is roughly tetrahedral, but the visible absorption spectra of the cobalt-substituted proteins¹² sometimes show substantially greater distortion from tetrahedral symmetry than is observed in simple four-coordinate complexes in solution.

The logical starting point for a comparative study is tetrahedral Co(ImH)₄²⁺, which can be formed in polar noncoordinating solvents such as acetone and nitromethane.⁹ The mixed ligand complex Co(ImH)₂Cl₂ provides an example with basic tetrahedral geometry,¹⁰ but with symmetry lowered to C_{2v} by virtue of the two different ligands. Chloride is not an ideal choice in this regard, but tetrahedral complexes with oxygen-containing ligands do not seem to be available.

A tetrahedral imidazolite complex, Co(Im)₄²⁻, is formed in water at high pH (13) in the presence of a large excess of imidazole.¹¹ This complex was included in this study because imidazolite coordination is of general interest, although it is unlikely that metal-bound imidazole is deprotonated at physiologically relevant pH values.¹¹ Unfortunately, the internal ligand modes of this complex could not be studied because they were swamped by the (1000-fold) excess ligand. A smaller excess led to formation of the insoluble imidazolite polymer, Co(Im)₂.^{10a,11} We also included the bishistidinate

complex of Co²⁺, in which imidazole is bound to the amino acid α -carbon atom. At neutral pH the complex is octahedral, with tridentate coordination via the imidazole, amine, and carboxylate groups.¹³ Because visible and ultraviolet absorption is weak for octahedral cobalt(II) complexes, little resonance enhancement is observed for this species. At high pH (>12.5) the complex is converted to a tetrahedral form with deprotonated imidazole and amine coordination.¹¹

Cobalt-Ligand Vibrational Modes. Excitation in the ligand-field absorption bands produced selective enhancement of low-frequency bands, attributable to cobalt-ligand stretching modes. The observed frequencies and assignments are listed in Table I. Co(ImH)₂Cl₂ showed all four cobalt-ligand modes (see inset, Figure 2), a symmetric pair (polarized) and an antisymmetric pair (depolarized). The two lower frequencies are assignable to cobalt-imidazole modes, as confirmed by the ~ 10 cm⁻¹ reductions in frequency for the 2-methylimidazole analogue (mass effect). Metal-imidazole frequencies are comparable to those of the pyridine analogue, Co(py)₂Cl₂¹⁴ (Table I), but lower than other metal-nitrogen stretching frequencies¹⁵ because of kinematic interactions with imidazole ring deformations. The cobalt-chloride frequencies correspond well with those of Co(py)₂Cl₂.

For the tetrahedral imidazole complexes only the antisymmetric stretch (depolarized) is observed (Figure 1). The frequency for Co(2MeImH)₄²⁺ is close to $\nu_{\text{Co-ImH(as)}}$ for Co(2MeImH)₂Cl₂. Likewise Co(1MeIm)₄²⁺ has a similar frequency. That of the simple imidazole complex, Co(ImH)₄²⁺, is substantially higher, however, at 301 cm⁻¹. The 27-cm⁻¹ increase over $\nu_{\text{Co-ImH(as)}}$ for Co(ImH)₂Cl₂ suggests an appreciable stronger Co-ImH bond. The increased charge on Co(ImH)₄²⁺ may be a factor. The charge effect would also apply to Co(2MeImH)₄²⁺ and Co(1MeIm)₄²⁺, but 2-MeImH may be sterically hindered, while 1-MeIm, with methylated nitrogen opposite the cobalt, is incapable of hydrogen bonding to the solvent (acetone or nitromethane). That hydrogen bonding may be a significant factor is further indicated by the observation that ν_{as} for Co(Im)₄²⁻ is only 5 cm⁻¹ higher than for Co(ImH)₄²⁺, although Im⁻, being a better donor than ImH,¹⁶ might be expected to have an appreciably stronger bond. The direction of hydrogen bonding is reversed in the two complexes: from ImH to acetone in Co(ImH)₄²⁺ and from water to Im⁻ in Co(Im)₄²⁻. This might compensate for intrinsic Co-imidazole bond strength differences.

Co(his)₂²⁻, which has deprotonated imidazole, shows a band at 305 cm⁻¹ (Figure 3), the same frequency as Co(Im)₄²⁻, assignable to $\nu_{\text{Co-Im(as)}}$. Chottard et al.¹⁷ assigned this band to an A₁ mode, but it is definitely depolarized. A weaker band, of uncertain polarization, is seen at 366 cm⁻¹ shifting to 356 cm⁻¹ in D₂O (the 305-cm⁻¹ band does not shift), which we assign to the symmetric Co-N stretch of the bound amine groups (compare $\nu_{\text{Ni-NH}_2(\text{as})} = 442$ cm⁻¹, shifting to 428 cm⁻¹ in D₂O, of square-planar Ni(glycine)₂).¹⁵ A 378-cm⁻¹ shoulder on the 366-cm⁻¹ band does not shift in D₂O, and

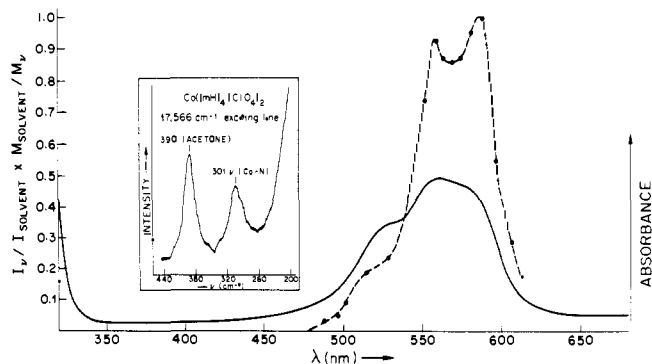


Figure 1. Absorption spectrum and excitation profile of the Co-Im asymmetric stretch in $\text{Co}(\text{ImH})_4(\text{ClO}_4)_2$. Insert: RR spectrum; conditions, spectral slit 8 cm^{-1} , time constant 3 s, scanning speed $0.5 \text{ cm}^{-1}/\text{s}$, sensitivity 10^3 Hz , concentration 9 mM. The excitation profile is plotted vs. $I_\nu / I_{\text{solvent}} \times M_{\text{solvent}} / M_\nu$ where I_ν and I_{solvent} are the intensities of the sample peak and the acetone peak at 390 cm^{-1} ; and M_{solvent} and M_ν are the molarities of the solvent and sample.

probably corresponds to a 370-cm^{-1} mode seen in histidine itself in 1 M NaOH.

No cobalt-ligand modes could be detected in octahedral $\text{Co}(\text{his})_2$ (neutral solution). The octahedral ligand field electronic transition¹¹ is too weak to provide resonance enhancement.

Ligand-Field Resonance Enhancement. In CoCl_4^{2-} ^{4b} and $\text{Co}(\text{NCS})_4^{2-}$ ^{4a} appreciable enhancement for the triply degenerate cobalt-ligand stretching mode, ν_3 , has been reported, but there is very little enhancement for the breathing mode, ν_1 . A vibronic (B term) scattering mechanism is therefore implicated,⁴ in which the intensity depends on vibronic mixing of the ligand-field transition with higher lying allowed transitions. Apparently the ligand-field transition is too weak to provide significant enhancement via the A term, which depends on the oscillator strength and origin shift of the resonant transition.¹⁸ In conformity with this inference, we were unable to detect the ν_1 Co-N stretching mode of either $\text{Co}(\text{ImH})_4^{2+}$ in acetone or $\text{Co}(\text{Im})_4^{2-}$ in water. A single low-frequency band is observed, at 301 and 306 cm^{-1} , respectively, assignable to ν_3 . It is essentially depolarized, with $\rho = 0.60$ and 0.65 for $\text{Co}(\text{Im})_4^{2-}$ and $\text{Co}(\text{ImH})_4^{2+}$. The slight reduction from 0.75 may reflect a reduction in effective molecular symmetry from T_d (rigorously tetrahedral symmetry is in any event not possible with imidazole ligands).

The excitation profile of the 301-cm^{-1} $\text{Co}(\text{ImH})_4^{2+}$ band is shown in Figure 1 along with the visible absorption band. The complexity in the ligand-field absorption of tetrahedral Co^{2+} complexes is attributed to splittings in the d-d manifold by spin-orbit interactions.¹⁹ The excitation profile shows the same complexity, and resembles the absorption profile rather closely. The relative contributions of the spin-orbit components differ somewhat between the absorption band and the excitation profile.

A different situation is encountered in the lower symmetry $\text{Co}(\text{ImH})_2\text{Cl}_2$, in which all four metal-ligand stretching vibrations are enhanced. The two depolarized asymmetric stretching modes require B term scattering, while the two polarized symmetric modes can gain intensity from either the A or the B terms. In view of the weakness of A-term scattering in the regular tetrahedral complexes, a B-term mechanism is more probable. The reason that polarized scattering is subject to B-term enhancement in $\text{Co}(\text{ImH})_2\text{Cl}_2$, but not in $\text{Co}(\text{ImH})_4^{2+}$ or $\text{Co}(\text{Im})_4^{2-}$, is plausibly related to the reduction in symmetry to C_{2v} from (approximately) T_d . The breathing mode of a tetrahedral complex does not alter its shape and is not expected to be effective in coupling two electronic transitions. In a C_{2v} complex, however, the symmetric

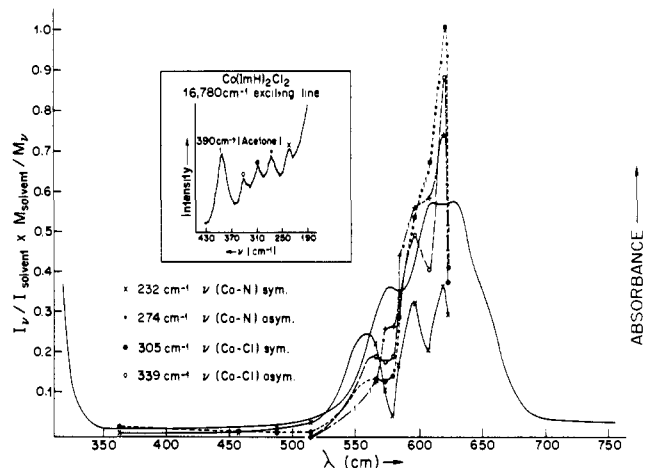


Figure 2. Absorption spectrum and excitation profile of all metal-ligand modes of $\text{Co}(\text{ImH})_2\text{Cl}_2$. Insert: RR spectrum; conditions, spectral slits 8 cm^{-1} , time constant 3 s, scanning speed $0.5 \text{ cm}^{-1}/\text{s}$, sensitivity 500 Hz, concentration 9 mM. The excitation profile is plotted as in Figure 1.

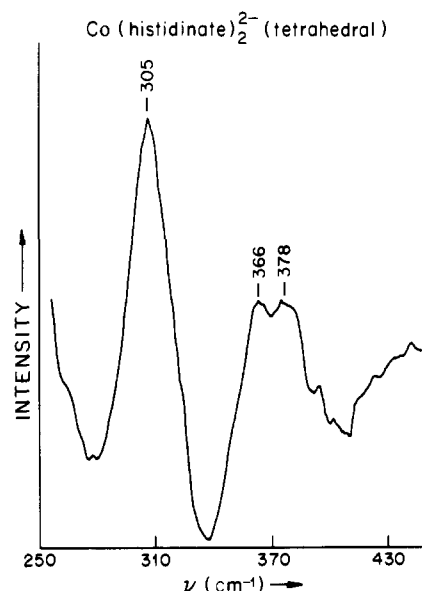


Figure 3. RR spectrum of $\text{Co}(\text{his})_2^{2-}$, using 5145-Å excitation. Data collected in a Nova 2/10 computer. Condition: spectral slit 10 cm^{-1} , time of data collection $5 \text{ s}/\text{cm}^{-1}$, number of scans 3, 13-point quadratic-cubic smooth. Frequencies and intensities were standardized with respect to the 983-cm^{-1} peak of SO_4^{2-} .

mode of each ligand pair (ImH or Cl) does change the shape of the molecule, and realigns the transition moments, thereby inducing vibronic mixing. This argument does not seem to apply to $\text{Co}(\text{his})_2^{2-}$, however, which also has approximate C_{2v} symmetry, with two imidazole and two amine ligands. In this case the asymmetric Co-Im mode is again dominant, and the symmetric counterpart is not seen. A Co-amine stretching mode is seen, but weakly. A possible explanation is that the ligand-field strengths of imidazole and amine are insufficiently different to show the pronounced symmetry lowering effect seen in $\text{Co}(\text{ImH})_2\text{Cl}_2$.

The excitation profiles of the four $\text{Co}(\text{ImH})_2\text{Cl}_2$ bands exhibit remarkable complexity, as seen in Figure 2. The visible absorption envelope is similar to that of $\text{Co}(\text{ImH})_4^{2+}$, but is shifted to longer wavelengths. Because of the limited dye laser tuning range, the excitation profiles extend only through the two highest energy absorption components. Nevertheless they are more highly structured than that of $\text{Co}(\text{ImH})_4^{2+}$, and show an extra peak, which is not evident in the absorption spectrum.

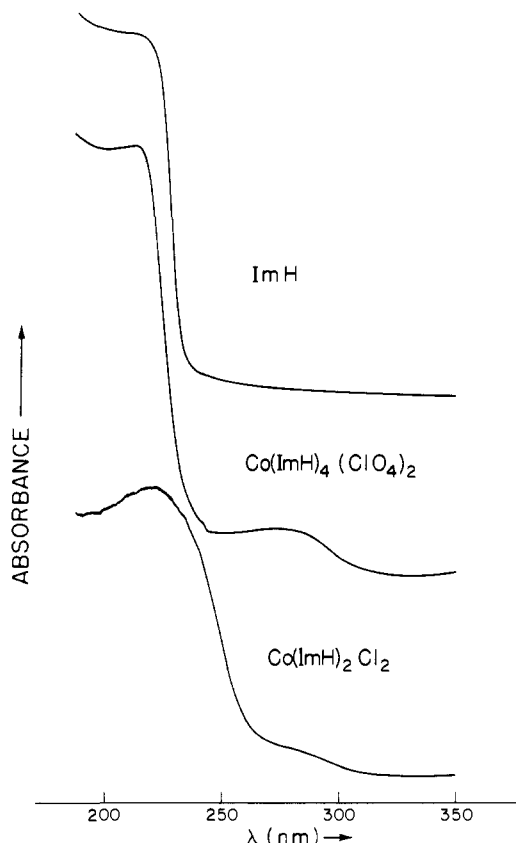


Figure 4. Absorption spectra of ImH, $\text{Co}(\text{ImH})_4(\text{ClO}_4)_2$, and $\text{Co}(\text{ImH})_2\text{Cl}_2$ as evaporated films on quartz plates. The spectra were recorded in a Cary 14 flushed with N_2 .

This may reflect a splitting of electronic levels due to symmetry lowering. It is not uncommon for Raman excitation profiles, which monitor individual vibrational modes, to show structure which is washed out in the absorption spectrum because of its composite vibronic character.²⁰

It is uncertain which allowed transition produces Raman intensity in the cobalt-ligand modes via the B term. The ligand field oscillator strength is generally thought to result from "d-p" mixing in the noncentrosymmetric complexes.¹⁹ This corresponds to mixing of the ligand field transitions with the higher energy cobalt-centered d-p transitions. Metal-ligand vibrations would be effective in mediating this mixing, with resonance enhancement of the associated Raman bands. There should be little discrimination among different ligands in a mixed ligand set. It is also possible that vibronic mixing with ligand \rightarrow metal charge transfer transitions induces both absorption and Raman intensity. In this case the Raman enhancement in mixed ligand complexes should be particularly marked for the ligand involved in the lowest energy charge transfer. The relative importance of d-p and charge transfer transitions is expected to depend on their energy separations from the ligand field transitions as well as on the vibronic integrals. The dominant mechanism may change from d-p to charge transfer mixing as ligands are bound which give rise to low energy charge transfer transitions.

Charge transfer transitions are expected in the ultraviolet for both imidazole and chloride.²¹ The UV spectrum of $\text{Co}(\text{ImH})_4^{2+}$ cannot be obtained in solution, because of solvent adsorption, but the spectrum of an evaporated film (Figure 4) shows a broad band at ~ 270 nm, beneath the intense imidazole absorption at 210 nm, also seen in free imidazole. $\text{Co}(\text{ImH})_2\text{Cl}_2$ has an absorption band at 240 nm in acetonitrile, but its evaporated film spectrum (Figure 4) shows an additional band at 270 nm. (Absorption at 240 nm is also seen but

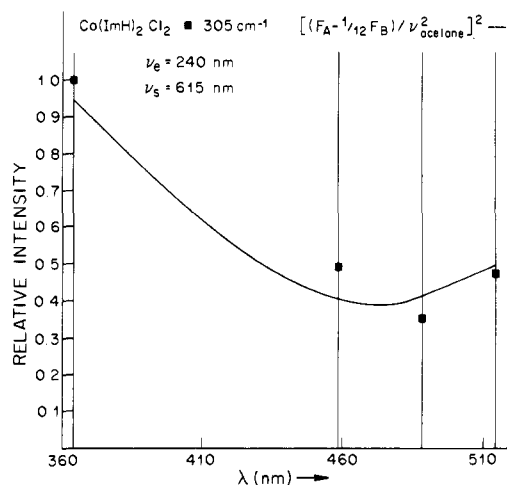


Figure 5. Observed and calculated excitation profile of the Co-Cl symmetric stretch in $\text{Co}(\text{ImH})_2\text{Cl}_2$. The calculation utilized the F_A and F_B frequency factors given by Albrecht and Hutley

$$F_A = \frac{\nu^2(\nu_e^2 + \nu_0^2)}{(\nu_e^2 - \nu_0^2)^2}$$

$$F_B = \frac{2\nu^2(\nu_e\nu_s + \nu_0^2)}{(\nu_e^2 - \nu_0^2)(\nu_s^2 - \nu_0^2)}$$

where ν_e and ν_s are the frequencies of the higher and lower energy electronic states, respectively, ν_0 is the frequency of the exciting laser line, and $\nu = \nu_0 - \Delta\nu$ where $\Delta\nu$ is the Raman frequency. The fit requires that the A and B terms add with opposite sign, with an F_A/F_B weighting ratio of 12. With the same sign, the upturn is abolished by destructive interference, the B term changing sign at resonance. A negative sign is possible for the B term if the vibronic mixing element is negative.

is unresolved from the 210-nm band.) We infer that the 270- and 240-nm absorptions arise from $\text{Im} \rightarrow \text{Co}$ and $\text{Cl} \rightarrow \text{Co}$ charge transfer transitions, respectively. Furlani's work²² on $\text{Co}(\text{thiourea})_2\text{Cl}_2$ complexes assigns a ~ 240 nm transition to $\text{Cl} \rightarrow \text{Co}(\text{II})$ charge transfer. In the case of $\text{Co}(\text{his})_2^{2-}$, the ultraviolet spectrum below 270 nm is obscured by the excess histidinate, but we expect that it contains an $\text{Im}^- \rightarrow \text{Co}(\text{II})$ charge transfer transition at much lower energy than the amine $\rightarrow \text{Co}(\text{II})$ transition. The observations that both Co-Cl and Co-Im modes are resonance enhanced in $\text{Co}(\text{ImH})_2\text{Cl}_2$, but that the Co-Im mode is dominant in $\text{Co}(\text{his})_2^{2-}$, is therefore suggestive of charge transfer mixing being the dominant vibronic mechanism. It is of interest that the excitation profiles of $\text{Co}(\text{ImH})_2\text{Cl}_2$ (Figure 2) show the symmetric Co-Cl mode to be slightly enhanced at 363.8 nm, while the symmetric Co-Im mode is not enhanced (the asymmetric modes are too weak to be measured in the UV). The off-resonance frequency dependencies for various scattering mechanisms can be estimated with the A and B term formulas given by Albrecht and Hutley²³ (Figure 5). It can be shown that 363.8 nm is too far away from either 270 nm or 240 nm to produce an upturn in the excitation profile from a pure B term that mixes the visible and near-UV transitions. The upturn in the Co-Cl profile implies an additional A term from one of the higher transitions. However, the upturn is too shallow to be modeled with an additional A term arising from the 270-nm transition. A fit to the data can be obtained with an A-term contribution from the 240-nm transition, as shown in Figure 5.

Bound Imidazole Modes. Figure 6 shows spectra of imidazole in H_2O (a) and in D_2O (b and c). Exchange of the N_1 proton is immediate in D_2O , while exchange of the C_2 proton is moderately rapid.¹⁶ Spectrum (b) was taken after dissolving ImH in D_2O at room temperature, while spectrum (c) was taken after heating at 65 °C for 6 h to ensure complete exchange of the C_2 protons. In this way we were able to identify frequency shifts for the N_1 and for the N_1 and C_2 deuterated

Table II

Aqueous solutions			Acetone- <i>d</i> ₆ solutions							Assignment ^a
ImH	ImH (N ₁ -D)	ImH (C ₂ -D + N ₁ -D)	ImH	ImH (N ₁ -D)	ImH (C ₂ -D + N ₁ -D)	Co(ImH) ₄ (ClO ₄) ₂		Co(ImH) ₂ - Cl ₂		
						N ₁ -D	C ₂ -D + N ₁ -D			
860 (br)	866 (br)	863								δ(R)
918	916	908								ω(C ₄ , C ₅ -H)
932 (sh)	956	950								δ(R)
1070	1072	1049								δ(R) + δ(C ₂ -H)
1100	1109	1096								δ(R) + δ(C ₄ , C ₅ -H)
1139	1136	1125	1142	1135	1126	1149	1139	1145	1149	δ(C ₄ , C ₅ -H) + δ(R)
1164						1181	1162	1168	1179	δ(R) + δ(N ₁ -H)
1260	1254	1163	1254	1253	1160	1257	1244	1215	1256	δ(C ₂ -H)
1330	1335	1310	1330	1323	1310	1336	1322	1318	1336	δ(R)
						1368 (vw)			1371 (vw)	
1431	1360	1355	1425	1356	1350	1440	1364	1365	1438	δ(N ₁ -H)
1490	1486	1454	1482	1480	1450	1511	1502	1433	1505	δ(R) + δ(C ₂ -H)
1535	1508	1508	1526	1505	1501	1554	1538	1530	1545	δ(R) + δ(N ₁ -H)

^a Based on ref 24 and 25, modified with regard to corrected deuterium shifts. δ(R), ring deformation; ω, out-of-plane deformation.

species. The starred bands in spectrum (b) are due to the latter species which had begun to form before the spectra were complete. Our data are in agreement with those of Perchard et al.,²⁴ except that the spectrum they report as belonging to the N₁ deuterated species is identical with our spectrum (c). Evidently their sample had been deuterated at C₂ as well as N₁.

The frequencies of the three isotopic species are listed in Table II, along with approximate assignments. The latter are based on the normal coordinate analysis of Colombo et al.,²⁵ modified with regard to the correct deuteration shifts. For example, the normal mode analysis, which utilized the deuteration data of Perchard et al., indicates major involvement of δN₁H (24% in the potential energy distribution) for the 1490-cm⁻¹ mode, but this frequency is affected by C₂, not by N₁ deuteration. Rather the 1535-cm⁻¹ mode shifts on N₁ deuteration.

Figure 7 shows spectra obtained with 363.8-nm excitation for ImH, Co(ImH)₄²⁺, and Co(ImH)₂Cl₂ in acetone-*d*₆ (acetone-*h*₆ has numerous interfering bands in the region of interest). Bands between 1100 and 600 cm⁻¹ are obscured by the solvent. The frequencies are correlated in Table II, and data for deuterated species are also given. Slight solvent shifts are seen for Im. The effects on the Im frequencies of coordination to Co²⁺ are subtle. The basic intensity pattern remains the same, the dominant band remaining at ~1255 cm⁻¹, with moderately strong bands at 1336 and 1149 cm⁻¹. A significant intensification occurs for the 1180-cm⁻¹ band, and a new band appears at 1368 cm⁻¹, which may correspond to the 1400-cm⁻¹ mode, seen weakly in the Raman spectrum of crystalline imidazole.²⁵

Frequency shifts on complexation are not large. The 1425-, 1482, and 1526-cm⁻¹ bands appear to increase by 15–30 cm⁻¹, but these bands, being relatively weak and broad, are difficult to characterize accurately. The intense 1255-cm⁻¹ band does not shift on coordination; a change in its normal mode composition is indicated, however, by the 13-cm⁻¹ shift induced upon N₁ deuteration in Co(ImH)₄²⁺ but not in free imidazole. This shift may be useful in distinguishing free and bound imidazole side chains in cobalt-substituted proteins.

The bound imidazole modes are not enhanced in the visible region but do show significant preresonance enhancement in the near UV. Figure 8 shows intensity data for the intense 1254-cm⁻¹ bands of Co(ImH)₄²⁺, Co(ImH)₂Cl₂, and of free imidazole in acetone-*d*₆. UV enhancement is greater for

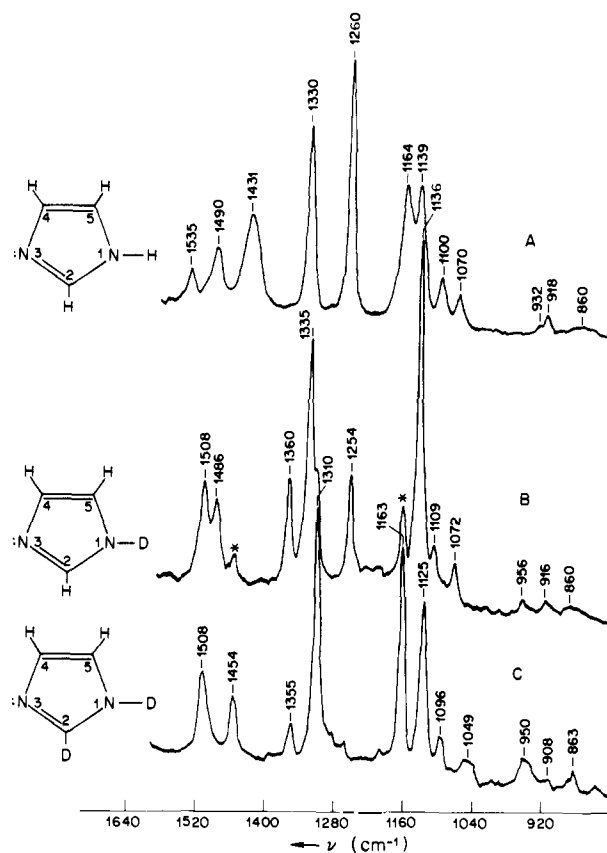


Figure 6. Raman spectra of (a) ImH, (b) Im(N₁-D), and (c) Im((C₂ + N₁)-D) in H₂O (a) and D₂O (b and c). Obtained with 4579-Å laser excitation. Conditions: spectral slit 10 cm⁻¹, time constant 3 s, scanning speed 1 cm⁻¹/s, sensitivity 5 × 10³ Hz, and concentrations ~2 M.

Co(ImH)₄²⁺ and Co(ImH)₂Cl₂ than for ImH (by a factor of 2.5 at 363.8 nm), but the rise is not steep enough to be accounted for by an A term involving only the 270-nm absorption band seen in the evaporated film spectrum. The data are fit, however (Figure 8), by summing A terms contributions from the 270- and 213-nm transitions and giving the latter a weight of 15/1. This ratio is not far from the ratio of absorptivities of the two transitions, suggesting that their Franck-Condon factors for the 1257-cm⁻¹ band are about the same. For free

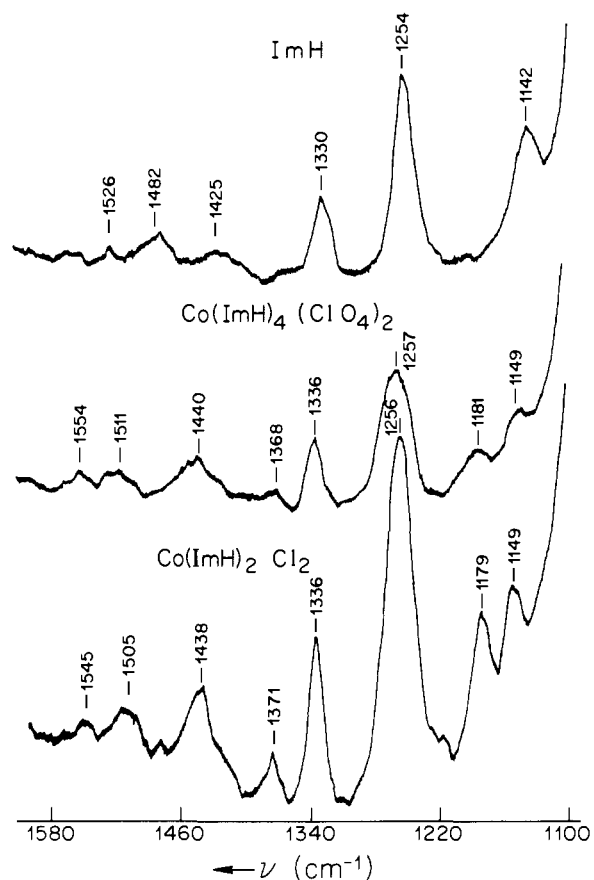


Figure 7. RR spectra of (a) ImH, (b) $\text{Co}(\text{ImH})_4(\text{ClO}_4)_2$, and (c) $\text{Co}(\text{ImH})_2\text{Cl}_2$ with 3638-Å laser excitation. Conditions: spectral slit (a, b, c) 12 cm^{-1} , time constant (a, b, c) 3 s, scanning speed (a, b, c) $1\text{ cm}^{-1}/\text{s}$, sensitivity (a) 10^3 Hz , (b and c) 500 Hz , concentration (a) 0.2 M (b and c) 50 mM, solvent acetone- d_6 .

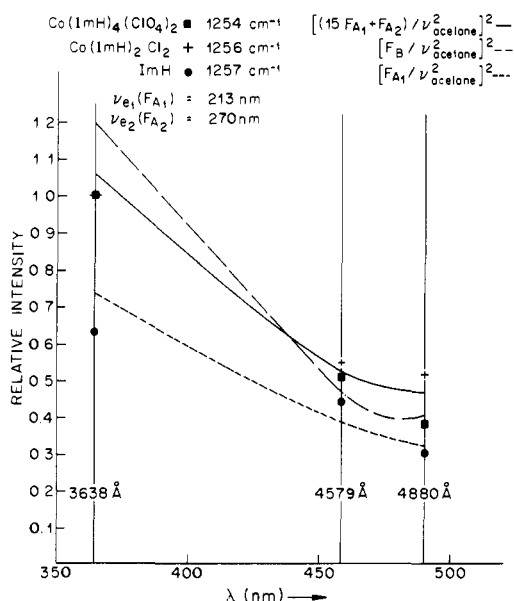


Figure 8. Observed and calculated excitation profile of the 1254-cm^{-1} band of $\text{Co}(\text{ImH})_4(\text{ClO}_4)_2$, $\text{Co}(\text{ImH})_2\text{Cl}_2$, and Im, in acetone- d_6 solution. The F_B term calculation used 213 and 270 nm as the high- and low-energy electronic states.

imidazole the enhancement is even weaker than is calculated from a 213-nm A term (Figure 8), suggesting that higher lying imidazole transitions²⁶ play a significant role.

Figure 9 shows 363.8-nm Raman spectra of octahedral $\text{Co}(\text{his})_2$ and tetrahedral $\text{Co}(\text{his})_2^{2-}$. Table III lists the ob-

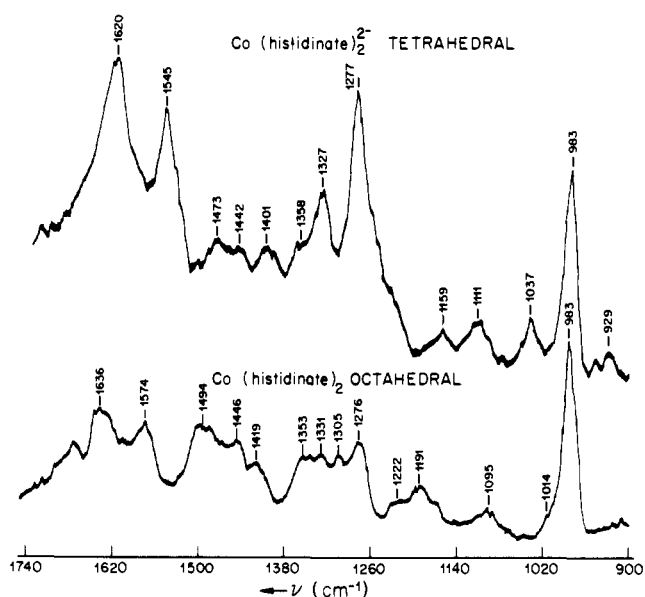


Figure 9. RR spectra of $\text{Co}(\text{his})_2$ and $\text{Co}(\text{his})_2^{2-}$, in H_2O with 3638-Å laser excitation. Conditions: spectral slit 12 cm^{-1} , time constant 3 s, scanning speed $1\text{ cm}^{-1}/\text{s}$, sensitivity 10^3 Hz , concentration 50 mM. All frequencies were standardized with the 983-cm^{-1} peak of SO_4^{2-} (0.1 M). The ratio of Co:his is 1:4.

Table III. Raman Frequencies for Histidine and Its Co(II) Complexes

	Histidine 4579 Å	$\text{Co}(\text{his})_2$ octahedral 3638 Å	$\text{Co}(\text{his})_2^{2-}$ tetrahedral 3638 Å
Im	1008	1014	1037
Im	1106	1095	1111
Im	1162 (br)	1191	1159
	1234	1222	1244
$\text{Im}\delta(\text{C}_2\text{-H})$	1267 ^a	1276 ^c	1277 ^e
	1288		
Im	1325	1305	
	1359	1331	1327
		1353	1358 (sh)
		1419	1401
		1446	
$\text{Im}\delta(\text{N}_1\text{-H})$	1440 ^b	1494 ^d	
			1442
			1473
$\nu(\text{COO})$	1491		
	1572	1574	1545
	1590 (sh)		
		~1620 (v br)	1620

^a $\Delta\nu$ for $(\text{N}_1\text{-H}/\text{N}_1\text{-D}) = 6\text{ cm}^{-1}$. $\Delta\nu$ for $(\text{N}_1\text{-H} + \text{C}_2\text{-H})/(\text{N}_1\text{-D} + \text{C}_2\text{-D}) = 30\text{ cm}^{-1}$. ^b $\Delta\nu$ for $(\text{N}_1\text{-H})/(\text{N}_1\text{-D}) = 63\text{ cm}^{-1}$. $\Delta\nu$ for $(\text{N}_1\text{-H} + \text{C}_2\text{-H})/(\text{N}_1\text{-D} + \text{C}_2\text{-D}) = \sim 63\text{ cm}^{-1}$. ^c $\Delta\nu$ for $(\text{N}_1\text{-H})/(\text{N}_1\text{-D}) = 9\text{ cm}^{-1}$. ^d $\Delta\nu$ for $(\text{N}_1\text{-H})/(\text{N}_1\text{-D}) = 70\text{ cm}^{-1}$. ^e $\Delta\nu$ for $(\text{N}_1\text{-H})/(\text{N}_1\text{-D}) = 0$. $\Delta\nu$ for $(\text{N}_1\text{-H} + \text{C}_2\text{-H})/(\text{N}_1\text{-D} + \text{C}_2\text{-D}) = 30\text{ cm}^{-1}$.

served frequencies along with those of free histidinate. The spectrum of $\text{Co}(\text{his})_2$ is complex and shows little selective enhancement. Frequency shifts in D_2O do serve to identify bands at 1277 and 1490 cm^{-1} with imidazole. The 1574-cm^{-1} mode is assignable to bound carboxylate.²⁷ The 1636-cm^{-1} band contains the NH_2 bending mode of the bound amine,²⁷ superimposed on the bending mode of water. It shifts to $\sim 1200\text{ cm}^{-1}$ in D_2O (cf. the analogous situation in $\text{Cu}(\text{II})\text{bisglycine}$).²⁷

The spectrum of $\text{Co}(\text{his})_2^{2-}$ is substantially resonance enhanced. In particular there is a two- to three-fold increase in the relative intensities of the bands at 1038, 1274, 1328, 1547,

and 1620 cm^{-1} between 457.9- and 363.8-nm excitation. The first three of these are attributable to imidazole. The 1620-cm^{-1} band shifts to $\sim 1200\text{ cm}^{-1}$ in D_2O , and is again a superposition of NH_2 and water bending modes. Its depolarization ratio of 0.6 indicates substantial δNH_2 contribution, a value of 0.2 being expected for the water mode. It is surprising, however, that δNH_2 is appreciably resonance enhanced. Even more surprising is the enhancement of the 1545-cm^{-1} band, which must be a carboxylate mode, shifted down from its value of 1574 cm^{-1} in the octahedral complex due to charge delocalization in the carboxylate group when it is *not* bound to cobalt. Enhancement of the δNH_2 and νCOO modes suggests preresonance with transitions involving the entire amino acid ligand, and not just imidazole.

Implications for Protein Studies. These results suggest that the prospects for observing Co-Im modes in Co^{2+} -substituted zinc proteins are good. From our intensity measurements (Figure 1) we estimate that the 301-cm^{-1} mode of $\text{Co}(\text{ImH})_4^{2+}$ is about 15 times as strong as the 983-cm^{-1} SO_4^{2-} ν_1 band, often used as an internal standard in aqueous protein studies. Similar enhancements are seen for the other complexes. Since 0.1 M SO_4^{2-} produces an acceptably strong reference signal, it should be possible to observe Co-Im modes at protein concentrations of 1–10 mM, in resonance with d-d bands about as strong as those found in tetrahedral Co^{2+} imidazole complexes. The spectra of $\text{Co}(\text{ImH})_2\text{Cl}_2$ and of $\text{Co}(\text{his})_2^{2-}$ suggest that other Co-ligand modes may also be detectable. Only asymmetric modes are expected to be observable, unless the effective symmetry is appreciably lower than tetrahedral.

The internal ligand modes offer less promise for monitoring cobalt-bound imidazole. Frequency shifts on binding are slight, and resonance enhancement, even in the near UV, is fairly weak. With 363.8-nm excitation the most intense imidazole mode in $\text{Co}(\text{ImH})_4^{2+}$, at 1257 cm^{-1} , is about 7.5 times stronger than the 983-cm^{-1} SO_4^{2-} band. It is only about three times stronger than the same mode of unbound imidazole, so that it would be difficult to distinguish imidazole in the coordination sphere of cobalt proteins from other imidazole side chains. This distinction may be possible, however, by measuring the spectrum in D_2O , since N_1 deuteration shifts the mode by 13 cm^{-1} in $\text{Co}(\text{ImH})_4^{2+}$, but leaves it essentially unshifted in unbound imidazole. Even greater discrimination

is possible via C_2 as well as N_1 deuteration, which produces a 55-cm^{-1} separation between the $\text{Co}(\text{ImH})_4^{2+}$ and ImH frequencies for this mode.

Acknowledgments. We thank Dr. Joan Valentine and Dr. Paul Stein for helpful discussions and Professor D. S. McClure for the use of the Cary 14 spectrometer. This work was supported by NIH Grant GM 13498.

References and Notes

- (1) B. L. Vallee and W. E. C. Wacker, "The Proteins", Vol. V, 2nd ed, H. Neurath, Ed., Academic Press, New York, N.Y., 1970.
- (2) (a) D. E. Drum, T. K. Li, and B. L. Vallee, *Biochemistry*, **8**, 3792 (1969); (b) P. L. Yeagle, C. H. Lochmuller, and R. W. Henkens, *Proc. Natl. Acad. Sci. U.S.A.*, **72**, 454 (1975).
- (3) C. M. Yoshida, T. B. Freedman, and T. M. Loehr, *J. Am. Chem. Soc.*, **97**, 1028 (1975).
- (4) (a) Y. M. Bosworth, R. J. H. Clark, and P. C. Turtle, *J. Chem. Soc., Dalton Trans.*, 2027 (1975); (b) G. Chottard and J. Bolard, *Chem. Phys. Lett.*, **33**, 309 (1975).
- (5) A. Liljas, K. K. Kannan, P. C. Bergstein, I. Waara, K. Fridborg, B. Strandberg, V. Carlboom, L. Jarup, S. Lovgren, and M. Petet, *Nature (London), New Biol.*, **235**, 131 (1972).
- (6) W. N. Lipscomb, J. A. Hartsuck, F. A. Quiocho, and G. N. Reeke, Jr., *Proc. Natl. Acad. Sci. U.S.A.*, **64**, 28 (1969).
- (7) B. W. Matthews, J. N. Jansonius, P. M. Colman, B. P. Schoenborn, and D. Duporque, *Nature (London), New Biol.*, **238**, 41 (1972).
- (8) H. Eklund, B. Nordstrom, E. Zeppezauer, G. Soderlund, I. Ohlsson, T. Boiwe, and C. I. Brandem, *FEBS Lett.*, **44**, 200 (1974).
- (9) W. J. Davis and J. Smith, *J. Chem. Soc. A*, 317 (1971).
- (10) (a) W. J. Eilbeck, F. Holmes, and A. E. Underhill, *J. Chem. Soc. A*, 757 (1967); (b) L. J. Antti and B. K. Lundberg, *Acta Chem. Scand.*, **26**, 3995 (1972).
- (11) P. J. Morris and R. B. Martin, *J. Am. Chem. Soc.*, **92**, 1543 (1970).
- (12) J. E. Coleman, *Biochemistry*, **4**, 2644 (1965).
- (13) R. Candlin and M. M. Harding, *J. Chem. Soc. A*, 384 (1970).
- (14) R. C. Clark, *Inorg. Chem.*, **4**, 350 (1965).
- (15) J. R. Kincaid and K. Nakamoto, *Spectrochim. Acta, Part A*, **32**, 277 (1976).
- (16) R. J. Sundberg and R. B. Martin, *Chem. Rev.*, **74**, 471 (1974).
- (17) G. Chottard and J. Bolard, *Inorg. Chim. Acta*, **20**, L17 (1976).
- (18) T. G. Spiro and P. Stein, *Annu. Rev. Phys. Chem.*, **28**, 501 (1977).
- (19) C. J. Ballhausen, "Introduction to Ligand Field Theory", McGraw-Hill, New York, N.Y., 1962.
- (20) B. P. Gaber, V. Miskowski, and T. G. Spiro, *J. Am. Chem. Soc.*, **96**, 6868 (1974).
- (21) C. K. Jorgensen, *Adv. Chem. Phys.*, **5**, 33 (1963).
- (22) O. Piovesana and C. Furlani, *J. Inorg. Nucl. Chem.*, **30**, 1249 (1968).
- (23) A. C. Albrecht and M. C. Hutley, *J. Chem. Phys.*, **55**, 4438 (1971).
- (24) C. Perchard, A. M. Bellocq, and A. Novak, *J. Chim. Phys. Phys.-Chim. Biol.*, **62**, 1349 (1965).
- (25) L. Colombo, P. Bleckman, B. Schrader, R. Schneider, and T. Plessner, *J. Chem. Phys.*, **61**, 3270 (1974).
- (26) I. Fischer-Hjalmars and J. Nag-Chandhuri, *Acta Chem. Scand.*, **23**, 2963 (1969).
- (27) R. A. Condrate and K. Nakamoto, *J. Chem. Phys.*, **42**, 2590 (1965).